Biological evaluation of some methyl 2-((4-acetylthiazol-2-yl)sulfanyl)-1,2,3,4-tetrahydro-6-methylpyrimidine-5-carboxylate derivatives as potential DHFR inhibitors to overcome antibiotic resistance

Sherkhan Pathan[1], Mazahar Farooqui[2], Suparna Deshmukh[3*]

[1]Department of Chemistry, Kohinoor Arts, Commerce and Science College Khultabad, Aurangabad, Maharashtra 431001, India; Email: sherkhanpathan01.91@gmail.com

[2]Department of Chemistry, Maulana Azad College of Arts, Science and Commerce, Aurangabad 431004, India; Email: mazahar_64@rediffmail.com

[*3]Department of Chemistry, S.K Gandhi College, Kada, Tal: Ashti, Dist: Beed, Maharashtra 414202, India; Email: suparna.deshmukh@gmail.com

Abstract

Multidrug-resistant bacteria are an increasing global threat. Current therapeutic medicines aren't enough to meet the demand. To address antibiotic resistance, new targets and inhibitors are needed. Dihydrofolate reductase (DHFR) is essential for bacterial development, hence DHFR inhibitors are helpful in treating bacterial infections. In the present work, we have designed some methyl 2-((4-acetylthiazol-2-yl)sulfanyl)-1,2,3,4-tetrahydro-6-methylpyrimidine-5-carboxylate as potential DHFR inhibitors through rational drug design approach. The designed derivatives were screened through Lipinski rule, Veber's rule, ADMET analysis, drug-likeness properties, and molecular docking. All of the compounds had action against gram-positive and gram-negative bacteria that was much more powerful than that of ampicillin. The majority of the compounds either had a higher potency than chloramphenicol or an equivalent potency to ciprofloxacin. Compound **C7** was sensitive at 25 µg/mL against *Escherichia coli, Pseudomonas aeruginosa,* and *Staphylococcus aureus* whereas compound **C20** was sensitive to all gram +ve and –ve bacteria at same concentration. Compound **C16** was sensitive at 50 µg/mL against all the bacteria. In antifungal activity, compound **C7** exhibited MFCs of 100 µg/mL against *Candida albicans*, *Aspergillus niger*, and *Aspergillus clavatus* which is same as Nystatin. Compound C16 and **C20** were also sensitive to all the antifungal strains at 100 or 200 µg/mL concentration. Compound **C20** is more potent than Greseofulvin against *Candida albicans*. As a result of our research, we came to the conclusion that compounds C7, C16, and C20 are the most effective and have the potential to be further developed into more promising molecules for the treatment of bacterial infections.

Keywords: DHFR, Biginelli reaction, Pyrimidines, Antibacterial, Molecular docking

Number: 10.14704/nq.2022.20.7.NQ33166 **Neuro Quantology 2022; 20(7):1343-1361**

1. Introduction

The advent of pathogens that are resistant to the vast majority of the conventional medicines used in treatment is now one of the most significant threats to the general population's health(Baig et al., 2022; Murali et al., 2014; Sánchez-Sánchez et al., 2017). The treatment of nosocomial infections, which pose a significant risk to public health on a global scale as a result of drug-resistant bacteria such as methicillin-resistant *Staphylococcus aureus* (MRSA) and multidrug-resistant *Escherichia coli*, is made extremely challenging as a result of these bacteria(Anwar et al., 2020; Jouhar et al., 2020; Loi et al., 2019). If we do nothing, a research commissioned by the United Kingdom Government estimates that "the cost in terms of lost global production between now and 2050 would be an astounding one hundred trillion USD." Infections caused by fungi may pose a significant threat to human health, and this is especially true for immunocompromised

patients. When it comes to clinical care, invasive fungal infections (IFIs) pose a significant challenge on a global scale(Indora and Kaushik, 2015; Marchese et al., 2016; Rahman et al., 2009). As a direct consequence of this, there is an increased emphasis placed on the need for new antimicrobial agents that are unique from the already available agents.

Since the middle of the 20th century, it has been shown that the dihydrofolate reductase (DHFR) enzyme may be used as a therapeutic target for the treatment of infections. DHFR plays a role in the production of raw material for cell proliferation in both prokaryotic and eukaryotic cells. This is accomplished by catalysing the reduction of dihydrofolate to tetrahydrofolate via the use of NADPH in the process. It is common practise to make use of DHFR inhibitors in the treatment of bacterial, fungal, and mycobacterial infections, as well as in the fight against malaria. Throughout the course of time, a wide variety of chemicals and medicines have been produced and made available on the market(He et al., 2020; Songsungthong et al., 2021; Wróbel et al., 2020).

Compounds that are based on the pyrimidine scaffold have been shown to display a wide variety of distinct biological functions, including antibacterial, antifungal, antiinflammatory, and anticancer properties(Mittersteiner et al., 2021; Nerkar, 2021; Verma et al., 2020). It has been shown that several derivatives based on amino pyrimidine have the ability to inhibit DHFR, which in turn results in antibacterial activity(Ahmed Elkanzi, 2020; Bhat et al., 2017). Because of this, the pyrimidine scaffold was chosen for the current work that we are doing in order to design and develop certain DHFR inhibitors as possible antibacterial and antifungal medicines. Calculations of ADMET characteristics were used to test the developed derivatives; those that were found to contain drug-like qualities were subsequently put via molecular docking research. After conducting spectral analysis and biological testing on the derivatives that showed considerable DHFR inhibitory potential, those compounds were then submitted to wet lab synthesis.

2. Material and Methods

2.1 Designing of Derivatives

In the present work, we have designed some methyl 2-((4-acetylthiazol-2-yl)sulfanyl)-1,2,3,4-tetrahydro-6-methylpyrimidine-5-carboxylate derivatives as illustrated in Table 1. After designing of derivatives, all the molecules were subjected for *in silico* screening to check drug-likeness properties.

Table 1. The designing approach of methyl 2-((4-acetylthiazol-2-yl)sulfanyl)-1,2,3,4-tetrahydro-6-methylpyrimidine-5-carboxylate derivatives

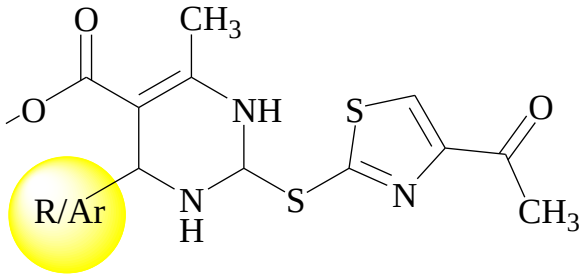

methyl 2-((4-acetylthiazol-2-yl)sulfanyl)-1,2,3,4-tetrahydro-6-methylpyrimidine-5-carboxylate derivatives

Compound code	Ar/R	Compound code	Ar/R
C1	—H	C11	—3-hydroxy phenyl
C2	—phenyl	C12	—2,3,4-trihydroxy phenyl
C3	—4-nitro phenyl	C13	—3-methoxy-4-hydroxy phenyl
C4	—4-bromo phenyl	C14	—2-methoxy phenyl

C5	—4-fluoro phenyl	C15	—4-styryl
C6	—4-chloro phenyl	C16	—napthyl
C7	—4-methyl phenyl	C17	—2,4-dinitro phenyl
C8	—4-methoxy phenyl	C18	—4-methylsulfonyl phenyl
C9	—4-hydroxy phenyl	C19	—4-dimethylamino phenyl
C10	—3-nitro phenyl	C20	—4-trifluoromethyl phenyl

2.2 Pharmacokinetics and toxicity predictions of designed derivatives

Utilizing molinspiration and SwissADME servers, Lipinski rule of five and pharmacokinetic features of developed derivatives were investigated(Kim et al., 2021)(Daina et al., 2017). An *in silico* toxicity prediction of designed derivatives has been made using ProTox-II, a webserver that is freely available(http://tox.charite.de/protox_II)(Banerjee et al., 2018).

2.3 Molecular Docking

After screening through *in silico* ADMET analysis, the screened molecules were subjected for the molecular docking studies. The proposed derivatives and the native ligand were docked against the crystal structure of the wild-type *E. coli* dihydrofolate reductase using Autodock vina 1.1.2 in PyRx 0.8(Dallakyan and Olson, 2015). ChemDraw Ultra 8.0 was used to draw the structures of the intended derivatives and native ligand (mole. File format). All the ligands were subjected for energy minimization by applying Universal Force Field (UFF)(Rappé et al., 1992). RCSB Protein Data Bank (PDB) entry 5CCC contains the wild-type *E. coli* dihydrofolate reductase complexed with 5,10-dideazatetrahydrofolate and oxidized nicotinamide adenine dinucleotide phosphate (https://www.rcsb.org/structure/5CCC). Discovery Studio Visualizer (version-19.1.0.18287) was used to refine the enzyme structure, purify it, and get it ready for docking(San Diego: Accelrys Software Inc., 2012). A three-dimensional grid box (size_x=39.7765672935Å; size_y=40.0725575009Å; size_z=35.1695000152Å) with an exhaustiveness value of 8 was created for molecular docking(Dallakyan and Olson, 2015). BIOVIA Discovery Studio Visualizer was used to locate the protein's active amino acid residues. The approach outlined by Khan et al. was used to perform the entire molecular docking procedure, identify cavity and active amino acid residues(Chaudhari et al., 2020; S. L. Khan et al., 2021; S.L. Khan et al., 2020; Sharuk L. Khan et al., 2020; Siddiqui et al., 2021). Fig. 1 shows the revealed cavity of DHFR with the co-crystallize ligand molecule.

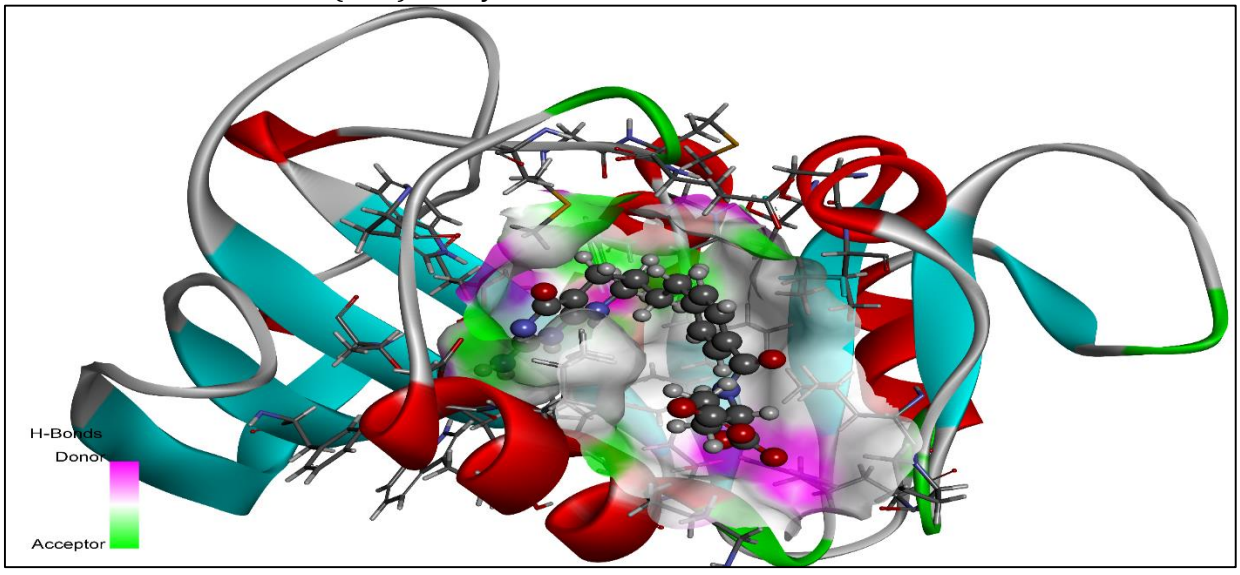

Fig. 1. 3D ribbon view of DHFR with native ligand in allosteric site

2.4 Reaction Scheme and Synthesis of selected derivatives

From *in silico* screening and molecular docking studies, compounds **C3, C7, C10, C16 and C20** were selected for the synthesis. All the required chemicals i.e. ethyl acetoacetate, aldehyde, thiourea, ferric chloride ($FeCl_3.6H_2O$), conc. HCl, ethanol, 4-chloropyrazole, potassium hydroxide (KOH), and acetone of synthetic grade were purchased and procured from Lab Trading Laboratory, Aurangabad, Maharashtra, India. The progress of the reaction was confirmed by Thin-layer chromatography [TLC, (Merck precoated silica GF 254)] and compounds were subjected for spectral analysis by ^1H, ^{13}C NMR (on a Varian-VXR-300S at 400 MHz NMR spectrometer) and Mass spectroscopy with chloroform (d_6) as the solvent and TMS as the internal standard; chemical shift values were expressed in δ ppm. The melting points were measured using the VEEGO MODEL VMP-D melting point apparatus. The detailed procedure for the synthesis of derivatives is discussed in the below section.

Step-I: Synthesis of 1,2,3,4-tetrahydropyrimidine-2-thiol

The reaction is a modified Biginelli reaction that generates 1,2,3,4-tetrahydropyrimidine-2-thiol from ethyl acetoacetate, aldehyde and thiourea[3,4]. A solution of ethyl acetoacetate (1.3gm, 10 mmol), thiourea (1.14gm, 15 mmol), ferric chloride ($FeCl_3.6H_2O$, 2.5 mmol) and conc. HCl (1-2 drops) in EtOH (20 mL) was heated independently with appropriate aldehydes (10 mmol), under reflux for 4-5 hrs[5]. After cooling, the reaction mixtures were poured onto crushed ice (100gm). Stirring was continued for several minutes, the solid products were filtered, independently washed with cold H_2O (2 times 50 mL) and a mixture of EtOH-H_2O, 1:1 (3 times 20 mL). The solids were dried and recrystallized from hot EtOH to afford pure products. The m.p. were recorded and are uncorrected. The yields obtained were in the range of 75-95%.

Step-II: Synthesis of final pyrimidine derivatives

1-(2-chlorothiazol-4-yl)ethanone (1.66 gm, 0.01 mol.) and 1, 2, 3, 4-tetrahydropyrimidine-2-thiols (0.01 mol.) were condensed by heating with Potassium hydroxide (KOH) and H_2O: Acetone (2:1) at about 50-60 ^{0}C for 45 min. Then the reaction mixture cooled to room temperature and then poured into ice-cold water, the precipitate was separated by filtration and recrystallized from ethanol. The yield was 90-95%. The proposed reaction scheme is illustrated in Fig. 2.

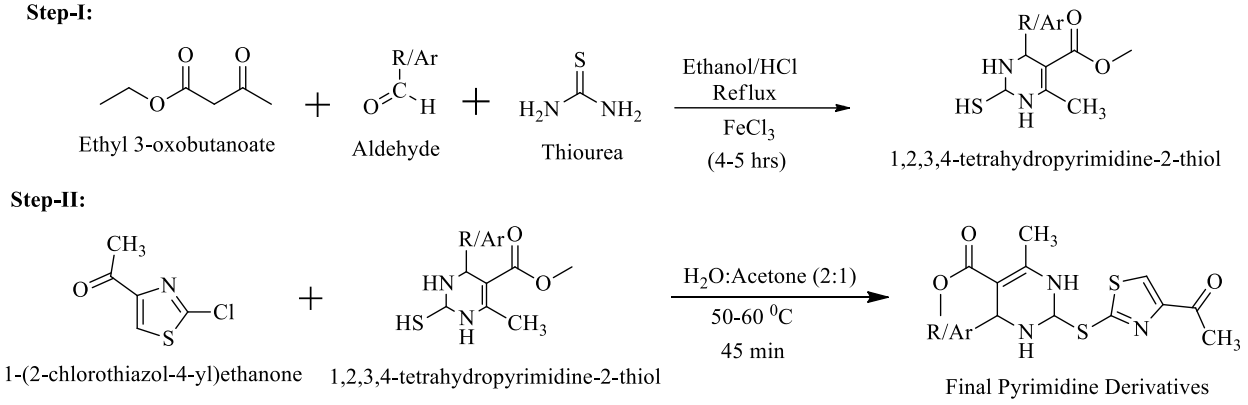

Fig. 2. The proposed reaction scheme for the synthesis of methyl 2-((4-acetylthiazol-2-yl) sulfanyl)-1,2,3,4-tetrahydro-6-methylpyrimidine-5-carboxylate derivatives

***Methyl2-((4-acetylthiazol-2-yl)sulfanyl)-1,2,3,4-tetrahydro-6-methyl-4-(4-nitrophenyl)pyrimidine-5-carboxylate* (C3)**

Molecular formula: $C_{18}H_{18}N_4O_5S_2$, molecular weight: 434.49 gm/mol, appearance: pale yellow solid, melting point: 209-211 ^{0}C, Rf value: 0.54, yield: 76%, solubility: ethanol, methanol, dichloromethane (DCM) and chloroform. Elemental analysis (*calc.*): C, 49.76; H, 4.18; N, 12.89; O, 18.41; S, 14.76. ^1H NMR ($CHCl_3$-d_6 400 MHz) δ ppm: 1.829 (s, methyl protons of pyrimidine), 2.135 (s, N-H of pyrimidine), 2.461 (s, methyl protons of phenyl ring), 3.671 (s, methoxy protons of acetate), 4.621, 4.701 (d, methylene protons of pyrimidine), 6.908 (s, phenyl protons), 7.834 (s, methylene protons of

diazole). ^{13}C NMR ($CHCl_3$-d_6 400 MHz) δ ppm: 15.980, 25.120, 52.901, 59.872, 76.902, 105.939, 106.001, 127.102, 128.582, 133.901, 136.291, 137.002, 154.091, 168.502. MS: m/z 435.23, 437.43 (m+1), 438.89 (m+2).

***methyl 2-((4-acetylthiazol-2-yl)sulfanyl)-1,2,3,4-tetrahydro-6-methyl-4-p-tolylpyrimidine-5-carboxylate* (C7)**

Molecular formula: $C_{19}H_{21}N_3O_3S_2$, molecular weight: 403.52 gm/mol, appearance: yellow, melting point: 205-207 ^{0}C, Rf values: 0.59, yield: 89%, solubility: ethanol, methanol, DCM, chloroform. Elemental analysis (*calc.*): C, 63.14; H, 5.30; N, 14.73; O, 8.41; S, 8.43. ^{1}H NMR ($CHCl_3$-d_6 400 MHz) δ ppm: 1.709 (s, methyl protons of pyrimidine), 2.205 (s, N-H of pyrimidine), 3.771 (s, methoxy protons of acetate), 4.671, 4.789 (d, methylene protons of pyrimidine), 6.908 (s, phenyl protons), 7.834 (s, methylene protons of diazole). 7.002, 7.128, 7.329, 7.571, 7.689, 7.790, 7.820, 7.981 (m, aromatic protons). ^{13}C NMR ($CHCl_3$-d_6 400 MHz) δ ppm: 14.003, 52.762, 56.990, 78.201, 104.891, 106.003, 124.201, 125.549, 126.889, 127.002, 128.652, 129.201, 132.781, 133.009, 134.310, 154.009, 168.980. MS: m/z 404.78, 406.34 (m+1), 410.67 (m+2).

***methyl 2-((4-acetylthiazol-2-yl)sulfanyl)-1,2,3,4-tetrahydro-6-methyl-4-(3-nitrophenyl)pyrimidine-5-carboxylate* (C10)**

Molecular formula: $C_{18}H_{18}N_4O_5S_2$, molecular weight: 434.49gm/mol, appearance: off-white, melting point: 264-266 ^{0}C, Rf value: 0.81, yield: 81%, solubility: ethanol, methanol, DCM, chloroform, benzene. Elemental analysis (*calc.*): C, 51.25; H, 4.30; F, 14.31; N, 14.06; O, 8.03; S, 8.05. ^{1}H NMR ($CHCl_3$-d_6 400 MHz) δ ppm: 1.698 (s, methyl protons of pyrimidine), 2.009 (s, N-H of pyrimidine), 3.799 (s, methoxy protons of acetate), 4.721, 4.798 (d, methylene protons of pyrimidine), 6.991 (s, phenyl protons), 7.392 (s, phenyl protons), 7.781 (s, methylene protons of diazole). ^{13}C NMR ($CHCl_3$-d_6 400 MHz) δ ppm: 16.029, 52.710, 58.892, 78.680, 104.630, 106.009, 122.128, 123.459, 124.903, 125.671, 126.582, 127.709, 128.430, 134.829, 142.302, 154.002, 168.992. MS: m/z 435.89, 437.21 (m+1), 440.79 (m+2).

***Methyl2-((4-acetylthiazol-2-yl)sulfanyl)-1,2,3,4-tetrahydro-6-methyl-4-(naphthalen-1-yl)pyrimidine-5-carboxylate* (C16)**

Molecular formula: $C_{22}H_{21}N_3O_3S_2$, molecular weight: 439.55gm/mol, appearance: white, melting point: 205-207 ^{0}C, Rf values: 0.39, yield: 84%, solubility: ethanol, methanol, DCM, chloroform. Elemental analysis (*calc.*): C, 63.14; H, 5.30; N, 14.73; O, 8.41; S, 8.43. ^{1}H NMR ($CHCl_3$-d_6 400 MHz) δ ppm: 1.709 (s, methyl protons of pyrimidine), 2.205 (s, N-H of pyrimidine), 3.771 (s, methoxy protons of acetate), 4.671, 4.789 (d, methylene protons of pyrimidine), 6.908 (s, phenyl protons), 7.834 (s, methylene protons of diazole), 7.002, 7.128, 7.329, 7.571, 7.689, 7.790, 7.820, 7.981 (m, aromatic protons). ^{13}C NMR ($CHCl_3$-d_6 400 MHz) δ ppm: 14.003, 52.762, 56.990, 78.201, 104.891, 106.003, 124.201, 125.549, 126.889, 127.002, 128.652, 129.201, 132.781, 133.009, 134.310, 154.009, 168.980. MS: m/z 441.56, 445.21 (m+1), 446.93 (m+2).

***Methyl 2-((4-acetylthiazol-2-yl) sulfanyl)-4-(4-(trifluoromethyl) phenyl)-1, 2, 3, 4-tetrahydro-6-methylpyrimidine-5-carboxylate* (C20)**

Molecular formula: $C_{19}H_{18}F_3N_3O_3S_2$, molecular weight: 457.49gm/mol, appearance: pale yellow, melting point: 189-191 ^{0}C, Rf values: 0.74, yield: 61%, solubility: ethanol, methanol, DCM, chloroform. ^{1}H NMR ($CHCl_3$-d_6 400 MHz) δ ppm: 1.709 (s, methyl protons of pyrimidine), 2.205 (s, N-H of pyrimidine), 3.771 (s, methoxy protons of acetate), 4.671, 4.789 (d, methylene protons of pyrimidine), 6.908 (s, phenyl protons), 7.834 (s, methylene protons of diazole), 7.002, 7.128, 7.329, 7.571, 7.689, 7.790, 7.820, 7.981 (m, aromatic protons). Elemental analysis (*calc.*): C, 49.88; H, 3.97; F, 12.46; N, 9.18; O, 10.49; S, 14.02. MS: m/z 458.34, 459.91 (m+1), 462.56 (m+2).

2.5 *In vitro* Biological Evaluation

Various concentrations of derivatives were prepared in DMSO to assess their antibacterial and antifungal activities against standard strains using broth dilution. Bacteria were maintained, and drugs were diluted in nutrient Mueller Hinton broth. The broth was inoculated with 10^8 colony-forming units (cfu) per milliliter of test strains (Institute of Microbial Technology, Chandigarh, India) determined by turbidity. Stock solutions of synthesized derivate (2 mg/mL) were serially diluted for primary and secondary screening. The primary screen included 1000, 500, and 250 µg/mL of synthesized derivatives, then those with activity

were further screened at 200, 100, 50, 25, 12.5, and 6.250 µg/mL. A control without antibiotic was sub-cultured (before inoculation) by spreading one loopful evenly over a quarter of a plate of medium suitable for growing test organisms and incubated at 37 ^{0}C overnight. The lowest concentrations of derivatives that inhibited bacterial or fungal growth were taken as minimal inhibitory concentrations (MICs). These were compared with the amount of control growth before incubation (original inoculum) to determine MIC accuracy. The standards for antibacterial activity were gentamycin, ampicillin, chloramphenicol, ciprofloxacin, and norfloxacin served, and those for antifungal activity were nystatin and griseofulvin. The antimalarial behavior was tested using plasmodium falciparum, with quinine and chloroquine as the standards. Both experiments took place at the Microcare laboratory and Tuberculosis Research Centre [TRC] in Surat, Gujarat(S. Khan et al., 2021; Shntaif et al., 2021; Siddiqui et al., 2021).

3. Results

The ability for researchers to explore the biological effects of potential pharmacological candidates is made feasible by pharmacokinetic features, which are an essential part of the drug development process(Khan et al., 2022). This compound's oral bioavailability was evaluated using Lipinski's rule of five and Veber's rules (Table 2). The ADME features of each of the suggested compounds were investigated in order to get a deeper comprehension of the pharmacokinetics profiles and drug-like qualities of each of the compounds (Table 3). The oral acute toxicity have been predicted along with LD_{50} (mg/kg), toxicity class, hepatotoxicity, carcinogenicity, immunotoxicity, mutagenicity, and cytotoxicity (Table 4). Table 5 lists the ligand energies (kcal/mol), docking scores (kcal/mol), active amino acids, bond length (Å), and different interactions of derivatives with DHFR. Table 6 depicts the most potent compounds' 2D and 3D docking orientations. The results of antimicrobial and antifungal activities of the synthesized derivatives are tabulated in Table 7 which shows the MICs and MFCs respectively.

Table 2. Lipinski rule of 5 and Veber's rule calculated for methyl 2-((4-acetylthiazol-2-yl)sulfanyl)-1,2,3,4-tetrahydro-6-methylpyrimidine-5-carboxylate derivatives

Compound Codes	Lipinski rule of five					Veber's rule	
	Log P	Mol. Wt.	HBA	HBD	Violations	Total polar surface area (Å^2)	No. of rotatable bonds
NL	0.70	443.45	7	6	2	187.50	10
C1	1.42	313.4	5	2	0	133.86	5
C2	2.59	389.49	5	2	0	133.86	6
C3	0.63	435.5	7	3	0	183.52	7
C4	3.18	468.39	5	2	0	133.86	6
C5	2.91	407.48	6	2	0	133.86	6
C6	3.13	423.94	5	2	0	133.86	6
C7	2.84	403.52	5	2	0	133.86	6
C8	2.59	419.52	6	2	0	143.09	7
C9	2.19	405.49	6	3	0	154.09	6
C10	0.66	435.5	7	3	0	183.52	7
C11	2.19	405.49	6	3	0	154.09	6
C12	1.44	437.49	8	5	0	194.55	6
C13	2.21	435.52	7	3	0	163.32	7
C14	2.58	419.52	6	2	0	143.09	7

C15	3.12	415.53	5	2	0	133.86	7
C16	3.47	439.55	5	2	0	133.86	6
C17	-2.48	481.5	9	4	1	233.18	8
C18	2.25	467.58	7	2	0	176.38	7
C19	2.65	432.56	5	2	0	137.1	7
C20	3.64	457.49	8	2	0	133.86	7

Where: NL, native ligand; Mol. Wt., molecular weight; HBA, hydrogen bond acceptors; HBD, hydrogen bond donors

Table 3. The pharmacokinetics and drug-likeness properties of developed compounds

Compound codes	Pharmacokinetics									Drug-likeness			
	GI abs.	BBB pen.	P-gp sub.	CYP1A2 inhibitors	CYP2C19 inhibitors	CYP2C9 inhibitors	CYP2D6 inhibitors	CYP3A4 inhibitors	Log K_p (skin permeation, cm/s)	Ghose	Egan	Muegge	Bioavailability Score
NL	Low	No	Yes	No	No	No	No	No	-8.81	0	1	1	0.11
C1	High	No	No	Yes	Yes	No	No	No	-6.99	0	1	0	0.55
C2	High	No	No	Yes	Yes	Yes	No	Yes	-6.25	0	1	0	0.55
C3	High	No	Yes	No	Yes	No	No	No	-6.98	0	1	1	0.55
C4	High	No	No	Yes	Yes	Yes	No	Yes	-6.25	0	1	0	0.55
C5	High	No	No	No	Yes	Yes	No	Yes	-6.29	0	1	0	0.55
C6	High	No	No	Yes	Yes	Yes	No	Yes	-6.02	0	1	0	0.55
C7	High	No	No	Yes	Yes	Yes	No	Yes	-6.08	0	1	0	0.55
C8	Low	No	No	No	Yes	Yes	No	Yes	-6.46	0	1	0	0.55
C9	Low	No	Yes	No	Yes	Yes	No	Yes	-6.6	0	1	1	0.55
C10	High	No	Yes	No	Yes	No	No	No	-6.98	0	1	1	0.55
C11	Low	No	Yes	No	Yes	Yes	No	Yes	-6.6	0	1	1	0.55
C12	Low	No	Yes	No	No	No	No	No	-7.3	0	1	1	0.55
C13	Low	No	Yes	No	Yes	Yes	No	Yes	-6.81	0	1	1	0.55
C14	Low	No	No	No	Yes	Yes	No	Yes	-6.46	0	1	0	0.55
C15	High	No	No	Yes	Yes	Yes	No	Yes	-5.95	0	1	0	0.55
C16	High	No	No	No	Yes	Yes	No	Yes	-5.67	0	1	0	0.55
C17	Low	No	Yes	No	No	No	No	No	-7.72	1	1	1	0.55
C18	Low	No	Yes	No	Yes	Yes	Yes	Yes	-7.27	0	1	1	0.55
C19	High	No	No	No	Yes	Yes	Yes	Yes	-6.43	0	1	0	0.55
C20	High	No	No	No	Yes	Yes	No	Yes	-6.04	0	1	0	0.55

Where: NL, Native ligand; GI abs., gastrointestinal absorption; BBB pen., blood brain barrier penetration; P-gp sub., p-glycoprotein substrate

Table 4. The predicted acute toxicities of the designed methyl 2-((4-acetylthiazol-2-yl)sulfanyl)-1,2,3,4-tetrahydro-6-methylpyrimidine-5-carboxylate derivatives

Compound codes	Parameters							
	LD_{50} (mg/kg)	Toxicity class	Prediction accuracy (%)	Hepatotoxicity (Probability)	Carcinogenicity (Probability)	Immunotoxicity (Probability)	Mutagenicity (Probability)	Cytotoxicity (Probability)
NL	135	3	67.38	I (0.87)	I (0.51)	I (0.99)	I (075)	I (0.63)
C1	1353	4	23	I (0.56)	I (0.52)	I (0.60)	I (0.64)	I (0.70)
C2	785	4	23	A (0.58)	I (0.51)	I (0.89)	I (0.64)	I (0.71)
C3	1000	4	23	A (0.58)	I (0.51)	I (0.89)	I (0.64)	I (0.71)
C4	300	3	23	A (0.61)	I (0.52)	A (0.50)	I (0.70)	I (0.67)
C5	785	4	23	A (0.62)	I (0.53)	A (0.55)	I (0.70)	I (0.71)7
C6	1000	4	23	A (0.60)	I (0.53)	I (0.59)	I (0.69)	I (0.73)
C7	785	4	23	A (0.58)	I (0.51)	I (0.91)	I (0.64)	I (0.71)
C8	785	4	23	A (0.56)	A (0.50)	I (0.74)	I (0.63)	I (0.74)
C9	1000	4	23	A (0.56)	A (0.50)	I (0.74)	I (0.63)	I (0.74)
C10	1000	4	23	A (0.58)	I (0.51)	I (0.91)	I (0.64)	I (0.71)
C11	785	4	23	A (0.56)	A (0.50)	A (0.66)	I (0.63)	I (0.74)
C12	150	3	23	A (0.55)	I (0.50)	A (0.84)	I (0.61)	I (0.76)
C13	3000	5	23	A (0.56)	I (0.50)	A (0.94)	I (0.60)	I (0.77)
C14	721	4	23	A (0.56)	A (0.51)	A (0.77)	I (0.61)	I (0.75)
C15	300	3	23	A (0.55)	I (0.52)	I (0.60)	I (0.66)	I (0.71)
C16	785	4	23	A (0.59)	I (0.50)	A (0.59)	I (0.55)	I (0.67)
C17	50	2	23	A (0.59)	I (0.50)	A (0.59)	I (0.55)	I (0.67)
C18	300	3	23	A (0.54)	I (0.58)	I (0.50)	I (0.71)	I (0.66)
C19	785	4	23	A (0.52)	I (0.53)	A (0.61)	I (0.59)	I (0.65)
C20	1500	4	23	A (0.61)	I (0.53)	I (0.63)	I (0.67)	I (0.71)

Where: NL, Native ligand; I, Inactive; A, Active

Table 5. The ligand energies (kcal/mol), docking scores (kcal/mol), active amino acids, bond length (Å), and different interactions of derivatives with DHFR

Active Amino acid	Bond Length	Bond Type	Bond Category	Ligand energy	Docking scores
Native ligand					
ASP27	1.88237	Hydrogen bond	Conventional hydrogen bond	209.71	-8.5
ASP27	2.19462				
ALA6	3.00495				
ILE5	1.91594				
ARG57	1.96549				
ARG57	2.17225				
ILE94	3.19208		Carbon hydrogen		

			bond		
ILE50	3.71343	Hydrophobic	Pi-Sigma		
PHE31	5.0747		Pi-Pi T-shaped		
PHE31	4.82737				
ILE94	4.98884		Alkyl		
ILE5	5.06209		Pi-Alkyl		
ALA7	4.05078				
C1					
ALA7	2.28772	Hydrogen Bond	Conventional Hydrogen Bond	432.07	-6.4
TRP22	2.42821				
GLY15	3.70656		Carbon Hydrogen Bond		
GLY15	3.52703				
MET20	4.93307	Hydrophobic	Pi-Alkyl		
LEU28	5.28478				
C2					
LEU24	2.32727	Hydrogen Bond	Conventional Hydrogen Bond	530.76	-7.6
TRP22	3.62021		Carbon Hydrogen Bond		
ASP27	3.85412	Electrostatic	Pi-Anion		
LEU28	5.2032	Hydrophobic	Pi-Alkyl		
ALA7	4.2804				
C3					
ASP27	2.41262	Hydrogen Bond	Conventional Hydrogen Bond	554.58	-8.6
LEU24	2.48735				
GLY15	3.55076		Carbon Hydrogen Bond		
ASN23	3.21742				
TRP30	3.52613				
LEU28	5.02679	Hydrophobic	Pi-Alkyl		
ALA7	4.119				
C5					
LEU24	2.56601	Hydrogen Bond	Conventional Hydrogen Bond	531.43	-8
ASN23	3.2209		Carbon Hydrogen Bond		
ASP27	3.16212	Halogen	Halogen (Fluorine)		
ASP27	3.5151				
ASP27	3.93493	Electrostatic	Pi-Anion		
LEU28	5.10431	Hydrophobic	Pi-Alkyl		
ALA7	4.30135				
C6					
LEU24	2.40062	Hydrogen Bond	Conventional Hydrogen Bond	547.06	-7.8
GLY15	3.47444		Carbon Hydrogen Bond		
ASN23	3.30937				
ASP27	4.0951	Electrostatic	Pi-Anion		
MET20	5.36121	Other	Pi-Sulfur		
TRP22	5.61176	Hydrophobic	Pi-Pi Stacked		
ILE5	4.60093		Alkyl		
LEU28	5.05881		Pi-Alkyl		
ALA7	4.31432				
TRP30	4.83822				

PHE31	5.09189				
C7					
LEU24	2.23137	Hydrogen Bond	Conventional Hydrogen Bond	529.29	-8.2
GLY15	3.66264		Carbon Hydrogen Bond		
TRP22	3.70748				
ASP27	4.0009	Electrostatic	Pi-Anion		
ILE5	4.53207	Hydrophobic	Alkyl		
LEU28	5.15542		Pi-Alkyl		
ALA7	4.23636				
TRP30	5.09803				
PHE31	5.07859				
C10					
ASP27	5.10776	Electrostatic	Attractive Charge	648.7	-8.1
GLU17	2.15529	Hydrogen Bond	Conventional Hydrogen Bond		
MET20	2.43123				
TYR100	2.97856				
ILE94	2.29654				
ALA7	2.43233				
ALA6	3.30873		Carbon Hydrogen Bond		
PHE31	3.99035	Hydrophobic	Pi-Sigma		
PHE31	5.02993		Pi-Pi T-shaped		
ALA7	4.325		Pi-Alkyl		
C15					
ARG57	2.25864	Hydrogen Bond	Conventional Hydrogen Bond	454.12	-7.5
ARG57	2.75432				
GLU17	3.6839	Electrostatic	Pi-Anion		
	3.79945	Hydrophobic	Pi-Sigma		
	5.75932		Pi-Pi Stacked		
PHE31	3.95392				
ILE94	4.98487		Pi-Alkyl		
C16					
LEU28	2.49359	Hydrogen Bond	Conventional Hydrogen Bond	493.17	-8.7
SER49	3.70697		Carbon Hydrogen Bond		
PHE31	2.86108		Pi-Donor Hydrogen Bond		
LEU28	3.69069	Hydrophobic	Pi-Sigma		
PHE31	4.14338		Pi-Pi Stacked		
PHE31	4.36071				
LYS32	5.12258		Pi-Alkyl		
ILE94	4.97108				
ALA7	4.91666				
C19					
ILE94	2.29243	Hydrogen Bond	Conventional Hydrogen Bond	565.22	-7.4
TYR100	2.70211				
ALA7	2.43084				
LEU28	3.64265		Carbon Hydrogen Bond		
PHE31	3.08585		Pi-Donor		

			Hydrogen Bond		
	3.86095	Hydrophobic	Pi-Sigma		
PHE31	5.01074		Pi-Pi Stacked		
LEU28	4.39564		Alkyl		
LYS32	4.24818				
ALA7	5.06539		Pi-Alkyl		
LEU28	5.09546				
LEU54	5.28722				
C20					
ALA6	2.89445	Hydrogen Bond;Halogen	Conventional Hydrogen Bond;Halogen (Fluorine)	550.63	-8.9
THR113	2.70302				
ALA7	3.51627	Hydrogen Bond	Carbon Hydrogen Bond		
TRP30	3.29513				
ILE5	3.68875	Halogen	Halogen (Fluorine)		
ALA6	3.01586				
ALA6	3.18544				
ASP27	3.61519				
ASP27	2.84991				
ASP27	2.93148				
ASP27	3.07368				
ILE5	4.53845	Hydrophobic	Alkyl		
ALA7	4.21032				
ILE50	4.60032		Pi-Alkyl		
ILE5	5.28292				
ALA7	4.64484				
TRP30	5.33577				

Table 6. The 2D- and 3D binding orientations of native ligand and molecules selected for the synthesis from virtual screening

2D-binding orientations	3D-binding orientations
Native ligand	
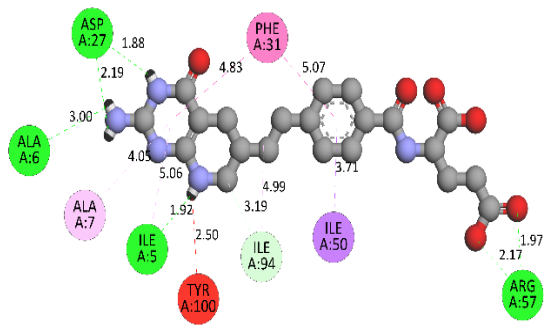	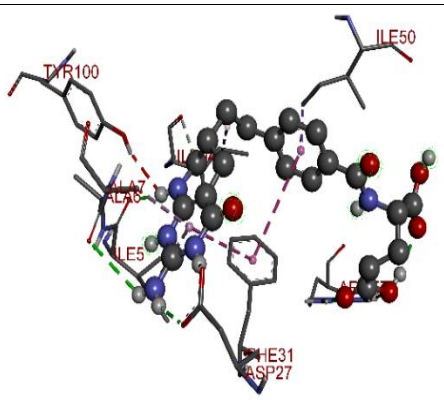
C1	

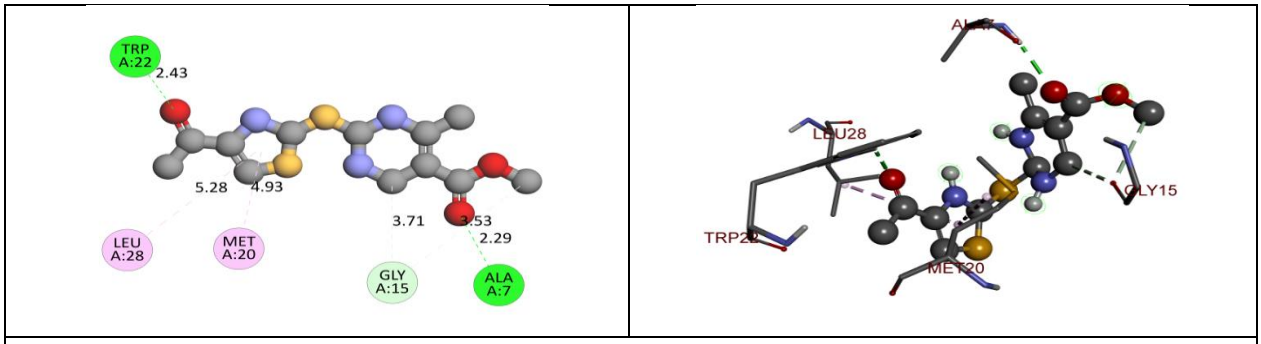
TRP A:22
2.43
5.28
4.93
LEU A:28
MET A:20
3.71
2.29
GLY A:15
ALA A:7
LEU28
GLY15
TRP22
MET20

C2

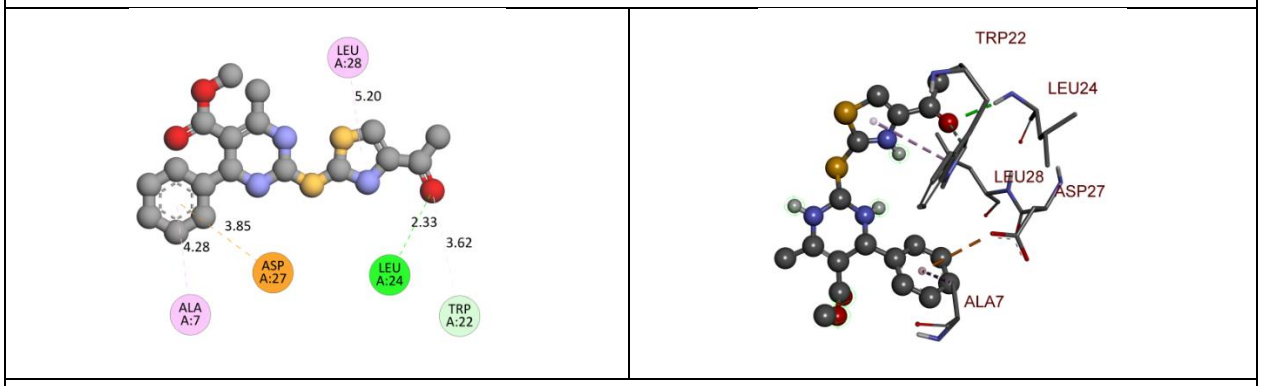
LEU A:28
5.20
3.85
4.28
2.33
3.62
ASP A:27
LEU A:24
ALA A:7
TRP A:22
TRP22
LEU24
LEU28
ASP27
ALA7

C3

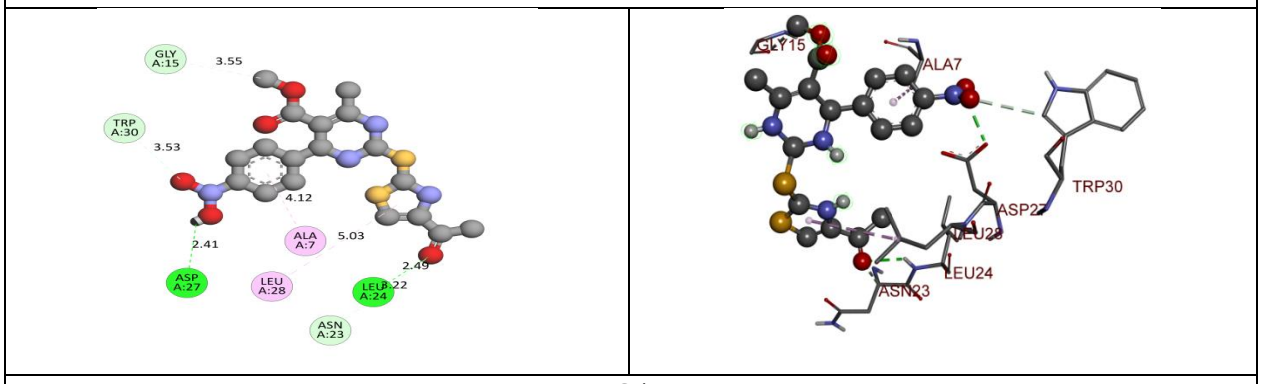
GLY A:15
3.55
TRP A:30
3.53
4.12
2.41
ALA A:7
5.03
2.49
ASP A:27
LEU A:28
LEU A:24
ASN A:23
GLY15
ALA7
TRP30
ASP27
LEU28
LEU24
ASN23

C5

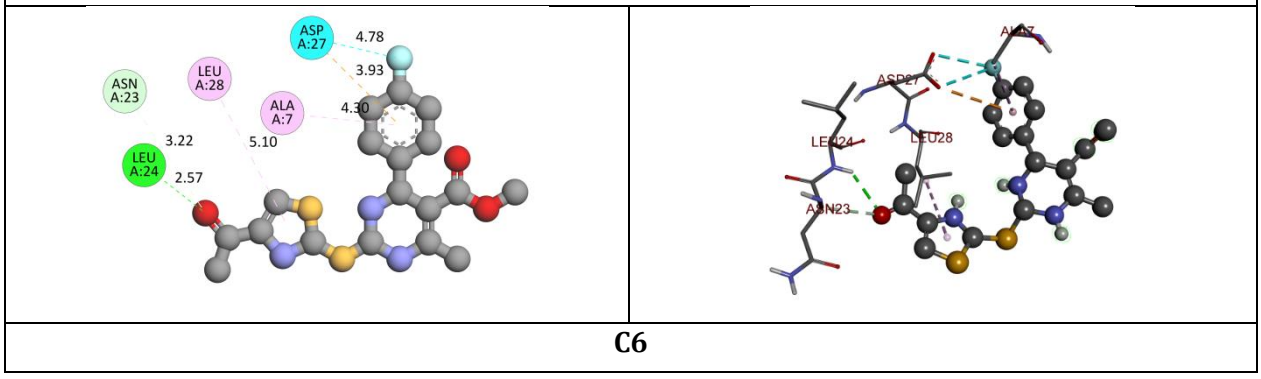
ASP A:27
4.78
3.93
ASN A:23
LEU A:28
ALA A:7
4.30
3.22
5.10
LEU A:24
2.57
LEU24
LEU28
ASN23

C6

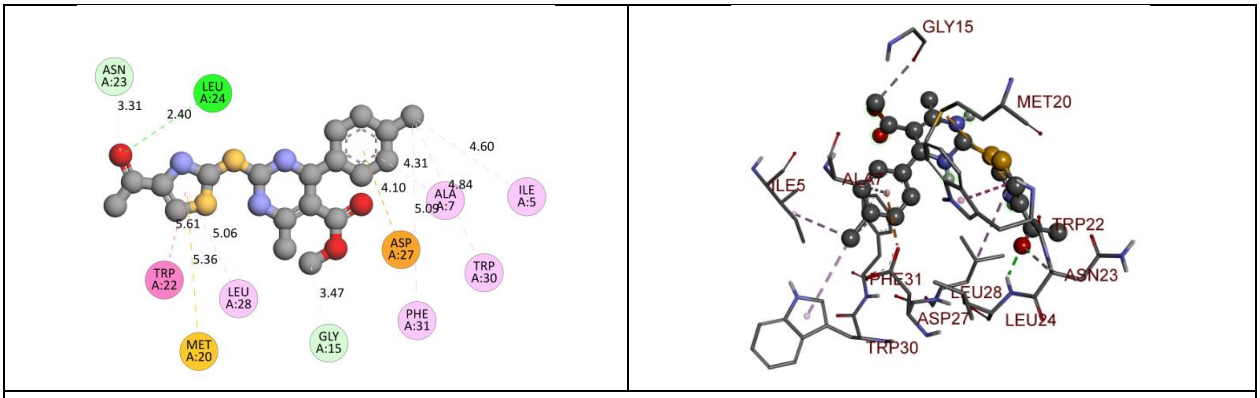

C7

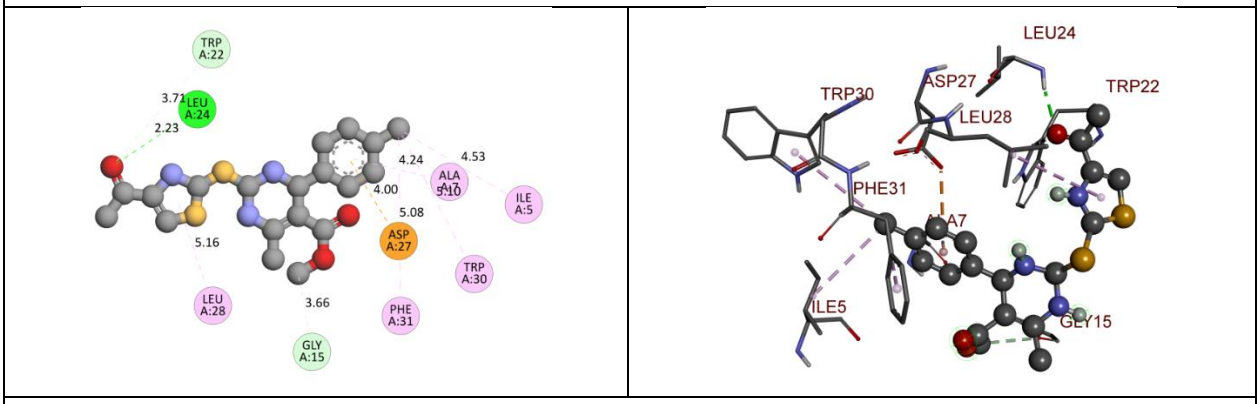

C10

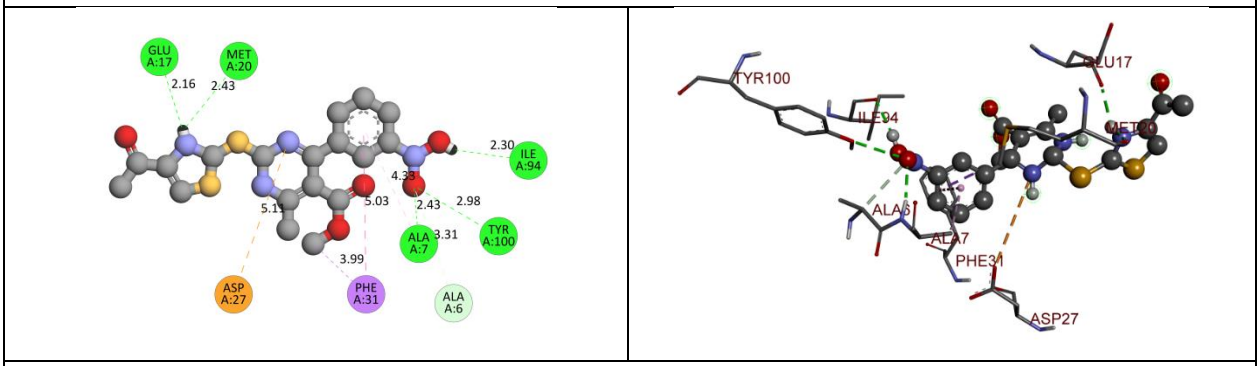

C15

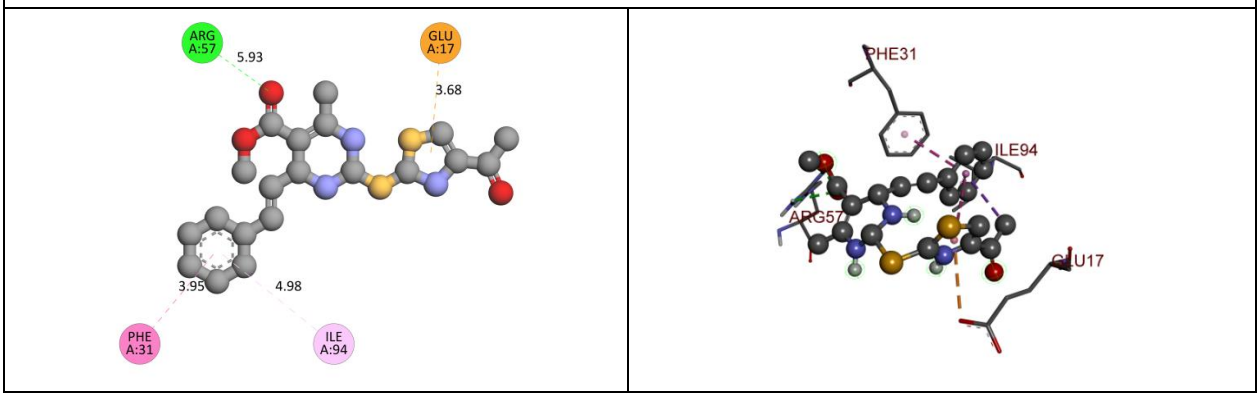

C16

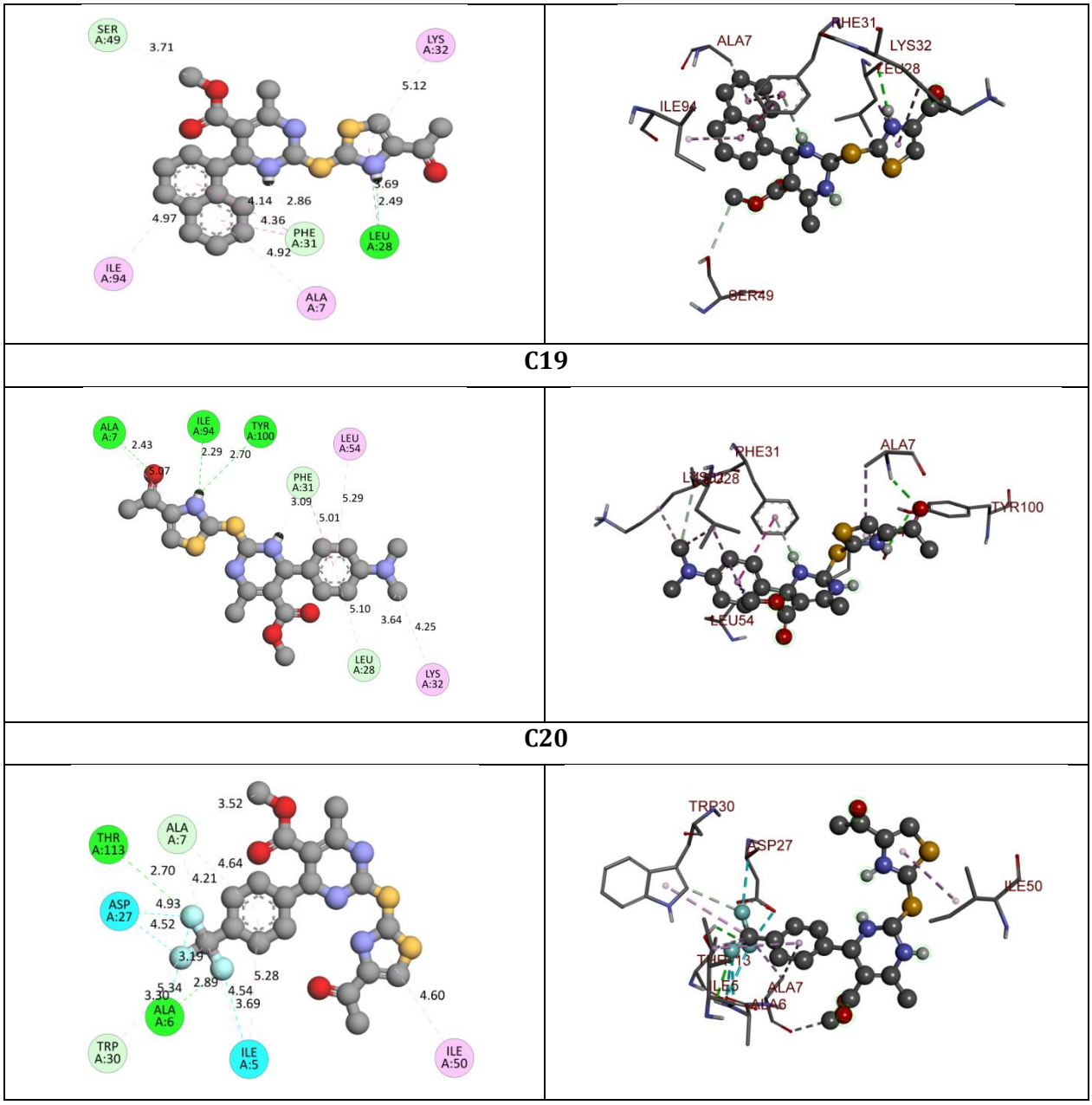

Table 7. The antimicrobial and antifungal activities of the synthesized derivatives

Compound code	Antimicrobial activity [*MIC* (µg/mL)]				Antifungal activity [*MFC* (µg/mL)]		
	E.C.	***P.A.***	***S.A.***	***S.P.***	***C.A.***	***A.N.***	***A.C.***
C3	25	25	25	50	100	100	100
C7	50	50	50	50	200	200	200
C10	25	25	25	25	100	200	100
C16	50	25	50	50	100	100	100
C20	50	25	50	50	100	100	100
Gentamycin	0.05	1	0.25	0.5	NA	NA	NA

Ampicillin	100	NA	250	100	NA	NA	NA
Chloramphenicol	50	50	50	50	NA	NA	NA
Ciprofloxacin	25	25	50	50	NA	NA	NA
Norfloxacine	10	10	10	10	NA	NA	NA
Nystatin	NA	NA	NA	NA	100	100	100
Greseofulvin	NA	NA	NA	NA	500	100	100

Where,

E.C., Escherichia coli; P.A., Pseudomonas aeruginosa; S.A., Staphylococcus aureus; S.P., Staphylococcus pyogenes; C.A., Candida albicans; A.N., Aspergillus niger; A.C., Aspergillus clavatus; MIC, Minimum inhibitory concentration; MFCs, minimum fungicidal concentration.

4. Discussion

In present study we have designed and developed some methyl 2-((4-acetylthiazol-2-yl)sulfanyl)-1,2,3,4-tetrahydro-6-methylpyrimidine-5-carboxylate derivatives as potential DHFR inhibitors. In accordance with Lipinski's and Veber's rule (Table 2), few molecules has violated both the rules. The log P values of all the molecules found between -2.48 to 3.64 which indicate optimum lipophilicity. Lipophilicity is a significant feature of the molecule that affects how it works in the body(S. Khan et al., 2021). It is determined by the compound's Log P value, which measures the drug's permeability in the body to reach the target tissue(Krzywinski and Altman, 2013; Lipinski et al., 2012). The molecular weight of all the molecules was below 500 Da which indicates active better transport of the molecules through biological membrane. Fortunately, the Lipinski rule of 5 had not been compromised by the compounds, excluding compound **C17**, which displayed 1 violation of Lipinski rule respectively(Khan et al., 2022; Shntaif et al., 2021). The total polar surface area (TPSA) and the number of rotatable bonds has been found to better discriminate between compounds that are orally active or not. According to Veber's rule, TPSA should be ≤ 140 and number of rotatable bonds should be ≤ 10. It was observed that native ligand violated the Veber's rule, as it has TPSA 187.50Å^2 and number of rotatable bonds 10 which indicate its poor oral bioavailability. Molecules **C8**, **C9**, **C12**, **C13** and **C18** has showed more TPSA than acceptable value therefore these compounds were indicated poor oral bioavailability.

In order to further optimize the compounds, pharmacokinetics and drug-likeness properties were calculated for each one. All the compounds including native ligand showed no penetration to the blood-brain barrier (BBB). The log *Kp* (skin penetration, cm/s) and bioavailability values of all the compounds were within acceptable limits. Few molecules and native ligand do not meet all, two, or one of the Ghose, Egan, and Muegge requirements (Table 3). Molecules **C8, C9, C11, C12, C13, C14, C17, C18** and native ligand exhibited low gastrointestinal (GI) absorption.

In acute toxicity predictions, one molecule i.e. **C17** falls in toxicity class-II [fatal if swallowed ($5<LD_{50}\leq50$)] whereas, native ligand and **C4, C12, C15 and C18** fall in toxicity class-III i.e. toxic if swallowed ($50<LD_{50}\leq300$). Molecules **C1, C2, C3, C5, C6, C7, C8, C9, C10, C11, C14, C16, C19 and C20** displayed toxicity class-IV which means harmful if swallowed ($300<LD_{50}\leq2000$). Molecule C13 showed toxicity class-V which indicate may be harmful if swallowed ($2000<LD_{50}\leq5000$)(Banerjee et al., 2018). From this virtual screening, it was concluded that compounds **C3**, C7, **C10**, **C16** and **C20** possess drug-like properties and hence were subjected to molecular docking studies.

The binding affinities of the derivatives have been compared with the binding mode of native ligand present in the crystal structure of DHFR (PDB ID: 5CCC). Native ligand exhibited -8.5 kcal/mol binding affinity with DHFR and formed 6 conventional hydrogen bonds with Asp27, Ala6, Ile5, Arg57, and one carbon-hydrogen bond with Ile94. It has developed many hydrophobic interactions such as Pi-sigma, Pi-Pi

T-shaped, alkyl, and Pi-alkyl bonds with Ile50, Phe31, Ile94, Ile5, and Ala7.

Compound **C1** exhibited -6.4 kcal/mol of binding affinity and formed two conventional hydrogen bonds and two carbon hydrogen bonds with Ala7, Trp22, and Gly15. It displayed one hydrophobic interaction (Pi-alkyl) with Met20 and Leu28. Compound **C2** exhibited -7.6 kcal/mol of binding affinity and formed one conventional hydrogen bond and one carbon hydrogen bond with Leu24 and Trp22. It displayed two hydrophobic interactions (Pi-alkyl) with Ala7 and Leu28 whereas formed one electrostatic (pi-anion) type of interactions with Asp27. Compound **C3** exhibited -8.6 kcal/mol of binding affinity and formed two conventional hydrogen bonds and two carbon hydrogen bonds with Asp27, Leu24, Gly15, Asn23 and Trp30. It displayed two hydrophobic interactions (Pi-alkyl) with Ala7 and Leu28.

Compound **C5** exhibited -8.6 kcal/mol of binding affinity and formed two conventional hydrogen bonds and two carbon hydrogen bonds with Asp27, Leu24, Gly15, Asn23 and Trp30. It displayed two hydrophobic interactions (Pi-alkyl) with Ala7 and Leu28. Compound **C6** showed -7.8 kcal/mol of binding affinity and formed one conventional hydrogen bond and two carbon hydrogen bonds with Leu24, Gly15 and Asn23. It displayed hydrophobic interactions (pi-pi stacked, alkyl, Pi-alkyl) with Trp22, Ile5, Leu28, Ala7, Trp30 and Phe31. Compound **C7** exhibited -8.2 kcal/mol of binding affinity and formed one conventional hydrogen bond and two carbon hydrogen bonds with Leu24, Gly15 and Asn23. It displayed hydrophobic interactions (pi-pi stacked, alkyl, Pi-alkyl) with Trp22, Ile5, Leu28, Ala7, Trp30 and Phe31. Compound **C10** showed -8.1 kcal/mol of binding affinity and formed five conventional hydrogen bonds and one carbon hydrogen bond with Glu17, Met20, Tyr100, Ile94, Ala7 and Ala6. It displayed hydrophobic interactions (pi-pi stacked, Pi-sigma, Pi-alkyl) with Phe31 and Ala7.

Compound **C15** exhibited -7.5 kcal/mol of binding affinity and formed two conventional hydrogen bonds with Arg57. It displayed hydrophobic interactions (pi-pi stacked, Pi-sigma, Pi-alkyl) with Phe31 and Ile94 whereas displayed electrostatic interactions (pi-anion) Glu17. Compound **C16** exhibited -8.7 kcal/mol of binding affinity and also formed one conventional hydrogen bond, one carbon hydrogen bond and pi-donor hydrogen bond with Leu28, Ser49 and Phe31. It displayed hydrophobic interactions (pi-pi stacked, Pi-sigma, Pi-alkyl) with Phe31, Lys32, Ile94 and Ala7. Compound **C19** exhibited -7.4 kcal/mol binding affinity and formed three conventional hydrogen bonds, carbon hydrogen bond , Pi-donor hydrogen bonds with Ile94,Tyr100,Ala7, Phe31.It displayed hydrophobic interactions (pi-pi stacked, Pi-sigma, alkyl, Pi-alkyl) with Phe31, Leu28, Lys32, Ala7, Leu54. Compound **C20** displayed -8.9 kcal/mol of binding affinity and formed two conventional hydrogen bonds with Ala6, Thr113, two carbon hydrogen bonds with Ala7, Trp30. It displayed hydrophobic interactions (pi-pi stacked, Pi-sigma, Pi-alkyl) with Ile5, Ala7, Ile50, Ile5, Ala7 and Trp30.

Millions of humans are now affected by bacterial diseases triggered by pathogenic bacteria which are responsible for elevated child mortality rates in developed countries [9]. Not all bacteria are pathogenic. For example, there are thousands of bacterial organisms in the human digestive tract, some of which are harmless and even useful. Furthermore, various mechanisms of action on the target site can aid in the discovery of potential drugs while developing antibacterial agents [10]. However, since bacteria have developed antibiotic tolerance, finding a new antibacterial agent became difficult. Gram-positive bacteria, such as *methicillin-resistant S. aureus, S. epidermis, vancomycin-resistant E. calcium,* and *penicillin-resistant S. pneumoniae*, induce the majority of bacterial infections. Fungal infections have become more frequent, and the majority of them are minor(Manohar et al., 2020). There are various varieties of fungi that cause infections today [12]. Species like *candida* and *aspergillus* are only a few examples(Liu et al., 2017). In present investigation, all the synthesized compounds were subjected for *in vitro* antibacterial and antifungal activity using different strains as given in Table 7.

All the synthesized compounds were sensitive to both gram +ve (*Staphylococcus aureus, Staphylococcus pyogenes*) and gram –ve (*Escherichia coli, Pseudomonas aeruginosa*) bacterial strains. All the compounds demonstrated more potent activity than Ampicillin against both gram-positive and gram-

negative bacteria. Most of the compounds were more or equipotent than Chloramphenicol and Ciprofloxacin. Compound **C7** was sensitive at 25 µg/mL against *Escherichia coli, Pseudomonas aeruginosa,* and *Staphylococcus aureus* whereas compound **C20** was sensitive to all gram +ve and –ve bacteria at same concentration. Compound **C16** was sensitive at 50 µg/mL against all the bacteria. In antifungal activity, compound **C7** exhibited MFCs of 100 µg/mL against *Candida albicans*, *Aspergillus niger*, and *Aspergillus clavatus* which is same as Nystatin. Compound **C16** and **C20** were also sensitive to all the antifungal strains at 100 or 200 µg/mL concentration. Compound **C20** is more potent than Greseofulvin against *Candida albicans*. It can be concluded that substitution at para position with bulky group can greatly increase the activity of the designed compounds.

5. Conclusion

Dihydrofolate reductase, often known as DHFR, is an essential enzyme that is necessary for bacteria to continue their development. As a result, inhibitors of DHFR have been shown to be effective antibacterial medicines in treating bacterial infections. In present study we have designed and developed some methyl 2-((4-acetylthiazol-2-yl)sulfanyl)-1,2,3,4-tetrahydro-6-methylpyrimidine-5-carboxylate derivatives as potential DHFR inhibitors. The developed derivatives were put through a series of tests, including molecular docking, ADMET analysis, drug-likeness qualities, and the Lipinski rule and Veber's rule. Synthesis of the chosen compounds was followed by in vitro biological testing to see how well they performed. As a result of our research, we came to the conclusion that compounds **C3, C7, C10, C16,** and **C20** are the most effective and have the potential to be further developed into more promising molecules for the treatment of bacterial infections.

References

Ahmed Elkanzi, N.A., 2020. Synthesis and Biological Activities of Some Pyrimidine Derivatives: A Review. Orient. J. Chem. 36, 1001–1015. https://doi.org/10.13005/ojc/360602

Anwar, K., Hussein, D., Salih, J., 2020. Antimicrobial susceptibility testing and phenotypic detection of MRSA isolated from diabetic foot infection. Int. J. Gen. Med. 13, 1349–1357. https://doi.org/10.2147/IJGM.S278574

Baig, M.S., Banu, A., Zehravi, M., Rana, R., Burle, S.S., Khan, S.L., Islam, F., Siddiqui, F.A., El, E., Massoud, S., Rahman, H., 2022. An Overview of Diabetic Foot Ulcers and Associated Problems with Special Emphasis on Treatments with Antimicrobials. Life 12, 1054.

Banerjee, P., Eckert, A.O., Schrey, A.K., Preissner, R., 2018. ProTox-II: A webserver for the prediction of toxicity of chemicals. Nucleic Acids Res. 46, W257–W263. https://doi.org/10.1093/nar/gky318

Bhat, A.R., Dongre, R.S., Naikoo, G.A., Hassan, I.U., Ara, T., 2017. Proficient synthesis of bioactive annulated pyrimidine derivatives: A review. J. Taibah Univ. Sci. 11, 1047–1069. https://doi.org/10.1016/j.jtusci.2017.05.005

Chaudhari, R.N., Khan, S.L., Chaudhary, R.S., Jain, S.P., Siddiqui, F.A., 2020. B-Sitosterol: Isolation from Muntingia Calabura Linn Bark Extract, Structural Elucidation And Molecular Docking Studies As Potential Inhibitor of SARS-CoV-2 Mpro (COVID-19). Asian J. Pharm. Clin. Res. 13, 204–209. https://doi.org/10.22159/ajpcr.2020.v13i5.37909

Daina, A., Michielin, O., Zoete, V., 2017. SwissADME: A free web tool to evaluate pharmacokinetics, drug-likeness and medicinal chemistry friendliness of small molecules. Sci. Rep. 7. https://doi.org/10.1038/srep42717

Dallakyan, S., Olson, A.J., 2015. Small-molecule library screening by docking with PyRx. Methods Mol. Biol. 1263, 243–250. https://doi.org/10.1007/978-1-4939-2269-7_19

Durga devi, D., Manivarman, S., Subashchandrabose, S., 2017. Synthesis, molecular characterization of pyrimidine derivative: A combined experimental and theoretical investigation. Karbala Int. J. Mod. Sci. 3, 18–28. https://doi.org/10.1016/j.kijoms.2017.01.001

He, J., Qiao, W., An, Q., Yang, T., Luo, Y., 2020. Dihydrofolate reductase inhibitors for use as antimicrobial agents. Eur. J. Med. Chem. 195. https://doi.org/10.1016/j.ejmech.2020.112268

Indora, N., Kaushik, D., 2015. Design ,

development and evaluation of ethosomal gel of fluconazole for topical fungal infection. Int. J. Eng. Sci. Invent. Res. Dev. I, 280–306.

Jouhar, L., Jaafar, R.F., Nasreddine, R., Itani, O., Haddad, F., Rizk, N., Hoballah, J.J., 2020. Microbiological profile and antimicrobial resistance among diabetic foot infections in Lebanon. Int. Wound J. 17, 1764–1773. https://doi.org/10.1111/iwj.13465

Khan, A., Unnisa, A., Sohel, M., Date, M., Panpaliya, N., Saboo, S.G., Siddiqui, F., Khan, S., 2022. Investigation of phytoconstituents of Enicostemma littorale as potential glucokinase activators through molecular docking for the treatment of type 2 diabetes mellitus. Silico Pharmacol. 10. https://doi.org/10.1007/s40203-021-00116-8

Khan, S., Kale, M., Siddiqui, F., Nema, N., 2021. Novel pyrimidine-benzimidazole hybrids with antibacterial and antifungal properties and potential inhibition of SARS-CoV-2 main protease and spike glycoprotein. Digit. Chinese Med. 4, 102–119. https://doi.org/10.1016/j.dcmed.2021.06.004

Khan, S.L., Siddiqui, F.A., Jain, S.P., Sonwane, G.M., 2020. Discovery of Potential Inhibitors of SARS-CoV-2 (COVID-19) Main Protease (Mpro) from Nigella Sativa (Black Seed) by Molecular Docking Study. Coronaviruses 2, 384–402. https://doi.org/10.2174/2666796701999200921094103

Khan, S.L., Siddiqui, F.A., Shaikh, M.S., Nema, N. V., Shaikh, A.A., 2021. Discovery of potential inhibitors of the receptor-binding domain (RBD) of pandemic disease-causing SARS-CoV-2 Spike Glycoprotein from Triphala through molecular docking. Curr. Chinese Chem. 01. https://doi.org/10.2174/2666001601666210322121802

Khan, Sharuk L., Sonwane, G.M., Siddiqui, F.A., Jain, S.P., Kale, M.A., Borkar, V.S., 2020. Discovery of Naturally Occurring Flavonoids as Human Cytochrome P450 (CYP3A4) Inhibitors with the Aid of Computational Chemistry. Indo Glob. J. Pharm. Sci. 10, 58–69. https://doi.org/10.35652/igjps.2020.10409

Kim, S., Chen, J., Cheng, T., Gindulyte, A., He, J., He, S., Li, Q., Shoemaker, B.A., Thiessen, P.A., Yu, B., Zaslavsky, L., Zhang, J., Bolton, E.E., 2021. PubChem in 2021: New data content and improved web interfaces. Nucleic Acids Res. 49, D1388–D1395. https://doi.org/10.1093/nar/gkaa971

Krzywinski, M., Altman, N., 2013. Points of significance: Significance, P values and t-tests. Nat. Methods 10, 1041–1042. https://doi.org/10.1038/nmeth.2698

Lipinski, C.A., Lombardo, F., Dominy, B.W., Feeney, P.J., 2012. Experimental and computational approaches to estimate solubility and permeability in drug discovery and development settings. Adv. Drug Deliv. Rev. https://doi.org/10.1016/j.addr.2012.09.019

Liu, Q., Meng, X., Li, Y., Zhao, C.N., Tang, G.Y., Li, H. Bin, 2017. Antibacterial and antifungal activities of spices. Int. J. Mol. Sci. 18. https://doi.org/10.3390/ijms18061283

Loi, V. Van, Huyen, N.T.T., Busche, T., Tung, Q.N., Gruhlke, M.C.H., Kalinowski, J., Bernhardt, J., Slusarenko, A.J., Antelmann, H., 2019. Staphylococcus aureus responds to allicin by global S-thioallylation – Role of the Brx/BSH/YpdA pathway and the disulfide reductase MerA to overcome allicin stress. Free Radic. Biol. Med. 139, 55–69. https://doi.org/10.1016/j.freeradbiomed.2019.05.018

Manohar, P., Loh, B., Athira, S., Nachimuthu, R., Hua, X., Welburn, S.C., Leptihn, S., 2020. Secondary Bacterial Infections During Pulmonary Viral Disease: Phage Therapeutics as Alternatives to Antibiotics? Front. Microbiol. 11. https://doi.org/10.3389/fmicb.2020.01434

Marchese, A., Barbieri, R., Sanches-Silva, A., Daglia, M., Nabavi, S.F., Jafari, N.J., Izadi, M., Ajami, M., Nabavi, S.M., 2016. Antifungal and antibacterial activities of allicin: A review. Trends Food Sci. Technol. 52, 49–56. https://doi.org/10.1016/j.tifs.2016.03.010

Mittersteiner, M., Farias, F.F.S., Bonacorso, H.G., Martins, M.A.P., Zanatta, N., 2021. Ultrasound-assisted synthesis of pyrimidines and their fused derivatives: A review. Ultrason. Sonochem. 79. https://doi.org/10.1016/j.ultsonch.2021.105683

Mohana Roopan, S., Sompalle, R., 2016. Synthetic chemistry of pyrimidines and fused pyrimidines: A review. Synth. Commun. 46, 645–672. https://doi.org/10.1080/00397911.2016.1165254

Murali, T.S., Kavitha, S., Spoorthi, J., Bhat, D. V.,

Prasad, A.S.B., Upton, Z., Ramachandra, L., Acharya, R. V., Satyamoorthy, K., 2014. Characteristics of microbial drug resistance and its correlates in chronic diabetic foot ulcer infections. J. Med. Microbiol. 63, 1377–1385. https://doi.org/10.1099/jmm.0.076034-0

Nerkar, A.U., 2021. Use of Pyrimidine and Its Derivative in Pharmaceuticals: A Review. J. Adv. Chem. Sci. 7, 729–732. https://doi.org/10.30799/jacs.239.21070203

Qin, H.L., Zhang, Z.W., Lekkala, R., Alsulami, H., Rakesh, K.P., 2020. Chalcone hybrids as privileged scaffolds in antimalarial drug discovery: A key review. Eur. J. Med. Chem. 193. https://doi.org/10.1016/j.ejmech.2020.112215

Rahman, M., Hasan, M.F., Das, R., Khan, A., 2009. The Determination of Antibacterial and Antifungal Activities of Polygonum hydropiper (L.) Root Extract. Adv. Biol. Res. (Rennes). 3, 53–56.

Rappé, A.K., Casewit, C.J., Colwell, K.S., Goddard, W.A., Skiff, W.M., 1992. UFF, a Full Periodic Table Force Field for Molecular Mechanics and Molecular Dynamics Simulations. J. Am. Chem. Soc. 114, 10024–10035. https://doi.org/10.1021/ja00051a040

Reta, A., Bitew Kifilie, A., Mengist, A., 2019. Bacterial Infections and Their Antibiotic Resistance Pattern in Ethiopia: A Systematic Review. Adv. Prev. Med. 2019, 1–10. https://doi.org/10.1155/2019/4380309

San Diego: Accelrys Software Inc., 2012. Discovery Studio Modeling Environment, Release 3.5. Accelrys Softw. Inc.

Sánchez-Sánchez, M., Cruz-Pulido, W.L., Bladinieres-Cámara, E., Alcalá-Durán, R., Rivera-Sánchez, G., Bocanegra-García, V., 2017. Bacterial Prevalence and Antibiotic Resistance in Clinical Isolates of Diabetic Foot Ulcers in the Northeast of Tamaulipas, Mexico. Int. J. Low. Extrem. Wounds 16, 129–134. https://doi.org/10.1177/1534734617705254

Sanchez, E., Doron, S., 2016. Bacterial Infections: Overview, in: International Encyclopedia of Public Health. pp. 196–205. https://doi.org/10.1016/B978-0-12-803678-5.00030-8

Shen, Z.L., Xu, X.P., Ji, S.J., 2010. Brønsted base-catalyzed one-pot three-component Biginelli-type reaction: An efficient synthesis of 4,5,6-triaryl-3,4-dihydropyrimidin-2(1H)-one and mechanistic study. J. Org. Chem. 75, 1162–1167. https://doi.org/10.1021/jo902394y

Shntaif, A.H., Khan, S., Tapadiya, G., Chettupalli, A., Saboo, S., Shaikh, M.S., Siddiqui, F., Amara, R.R., 2021. Rational drug design, synthesis, and biological evaluation of novel N-(2-arylaminophenyl)-2,3-diphenylquinoxaline-6-sulfonamides as potential antimalarial, antifungal, and antibacterial agents. Digit. Chinese Med. 4, 290–304. https://doi.org/10.1016/j.dcmed.2021.12.004

Siddiqui, F.A., Khan, S.L., Marathe, R.P., Nema, N. V., 2021. Design, Synthesis, and In Silico Studies of Novel N-(2-Aminophenyl)-2,3-Diphenylquinoxaline-6-Sulfonamide Derivatives Targeting Receptor- Binding Domain (RBD) of SARS-CoV-2 Spike Glycoprotein and their Evaluation as Antimicrobial and Antimalarial Agents. Lett. Drug Des. Discov. 18, 915–931. https://doi.org/10.2174/1570180818666210427095203

Songsungthong, W., Prasopporn, S., Bohan, L., Srimanote, P., Leartsakulpanich, U., Yongkiettrakul, S., 2021. A novel bicyclic 2,4-diaminopyrimidine inhibitor of Streptococcus suis dihydrofolate reductase. PeerJ 9. https://doi.org/10.7717/peerj.10743

Verma, V., Joshi, C.P., Agarwal, A., Soni, S., Kataria, U., 2020. A Review on Pharmacological Aspects of Pyrimidine Derivatives. J. Drug Deliv. Ther. 10, 358–361. https://doi.org/10.22270/jddt.v10i5.4295

Wróbel, A., Arciszewska, K., Maliszewski, D., Drozdowska, D., 2020. Trimethoprim and other nonclassical antifolates an excellent template for searching modifications of dihydrofolate reductase enzyme inhibitors. J. Antibiot. (Tokyo). 73, 5–27. https://doi.org/10.1038/s41429-019-0240-6